

Multi-Link and AUV-aided Energy-Efficient Underwater Emergency Response

Zhengrui Huang

Abstract—The recent development of wireless communication has provided many promising solutions to emergency response. To effectively realize the energy-efficient underwater emergency response and adequately harness merits of different underwater communication links (UCL), this article proposes an underwater emergency communication network (UECN) aided by multiple UCLs and autonomous underwater vehicles (AUV) to collect underwater emergency data. Specifically, we first select the optimal emergency response mode (ERM) for each underwater sensor node (USN) with the help of greedy searching and reinforcement learning (RL), and the “isolated” USNs (IUSN) can be found out. Second, based on the distribution of IUSNs, we dispatch AUVs to assist IUSNs in underwater communication by jointly solving the optimal AUV position and velocity, which can dramatically shorten the amount of time for data collection and motion. Finally, the best tradeoff between response efficiency and energy consumption is achieved by multiobjective optimization, where the amount of time for emergency response and the total energy consumption are simultaneously minimized, subject to a given set of transmit power, signal-to-interference-plus-noise ratio (SINR), outage probability, and energy constraints. Simulation results show that the proposed system significantly improves the response efficiency and overcomes the limitations of existing works, which makes contributions to emergency decision-making.

Index Terms—Wireless communication, emergency response, underwater communication link (UCL), reinforcement learning (RL), autonomous unmanned vehicle (AUV), multiobjective optimization.

I. INTRODUCTION

RECENT advancements in wireless communication have provided many potential solutions to the energy-efficient emergency response and made some contributions to post-disaster rescues, including monitoring industrial devices [1], evaluating environmental parameters [2], and recovering communication networks [3]. In practice, most works focus on above-ground emergency response [4], such as using a device-to-device (D2D)-based wireless sensor network (WSN) to provide emergency information for victims [5] or dispatching unmanned aerial vehicles (UAV) to collect data returned from ground WSNs (GWSN) [6]. However, studies on how to build a cost-efficient underwater emergency communication network (UECN) and overcome limitations of traditional transmission

media are relatively limited [7]. To realize energy-efficient underwater emergency response, it is important to fuse heterogeneous underwater communication links (UCL) and make full use of the mobility of unmanned vehicles (UV). In general, UCLs mainly include underwater light (UL), underwater acoustic (UA), and radio frequency (RF) links [8], through which underwater sensor nodes (USN) can transmit emergency data toward rear rescue centers. Furthermore, with the support of autonomous underwater vehicles (AUV) and unmanned surface vehicles (USV), USNs can directly transmit emergency data to gateways, namely, USVs (e.g., ships or buoys), or transfer data to underwater relay nodes or AUVs that are connected with gateways, so the rear emergency center can plan real-time rescue schemes via the collected information. Therefore, for energy-efficiency emergency response, the main challenges include joint UCL selection and optimization, relay selection, and UV deployment.

A. Related Works and Motivation

In [9], some promising fusion strategies were discussed, such as RF/visible light communication (VLC), RF/free-space optical (FSO), and acoustic/optical, but it is still unclear how to jointly fuse different UCLs and optimize UCL performance to realize energy-efficiency underwater emergency response, and it is worth noting that each kind of UCL has its own merits and demerits [10], as shown in Table I.

For UL links, they can provide high-data-rate wireless accesses within relatively short communication distances. In [11], Elamassie *et al.* derived the closed-form expression of bit error rate (BER) for vertical UL links. To expand the UL communication range, a light-path routing (LiPaR) protocol derived from beamwidth tradeoffs was proposed to optimize end-to-end (E2E) data rates [12]. However, these two works did not optimize the performance of UL links. In addition, an UL relay system was designed to approximate the USN outage probability [13], and Shihada *et al.* used an LED or laser to provide wireless accesses for underwater users at different distances [14]. For an UA link, acoustic communication can support up to 20 km underwater communication, which has wider communication coverage than other UCLs. In [15], Huang *et al.* proposed an adaptive modulation scheme for the best UA link selection, where the frequency is from 900 Hz to 1500 Hz. Following [15], to minimize the energy consumption of data transmission, a role assignment (RA)-based method was devised to optimize UA transmit power in [16], but this work was just suitable in static scenarios. From the perspective of quality of service (QoS), a cost-effective network was deployed

Zhengrui Huang is with the Academy of Digital China (Fujian), Fuzhou University, Fuzhou 350108, China, and the Key Laboratory of Spatial Data Mining & Information Sharing of Ministry Education, Fuzhou University, Fuzhou 350108, China.

to optimize acoustic links while supporting communication requirements (e.g., average delay and packet transmission error) [17]. For a RF link, radio waves can provide moderate transmission rates and have a unique propagation mechanism compared with UL or UA links. In [18], Saini *et al.* proposed a RF path loss (PL) model by taking into account temperature and salinity. Based on [18], Omeke *et al.* investigated the performance of RF links in freshwater and seawater [19], and the performances (e.g., delay, PL and outage probability) of RF signals at 433 MHz and 2.4 GHz were analyzed respectively in [20].

Following [11]–[20], it is clear that using single UCL is not robust, i.e., longer communication distance results in lower data rates, so some possible hybrid UCLs are promising [9]. In [21], an UL system combined with UA links was designed to offer high capacity with low latency. Inspired by [22], Johnson *et al.* investigated the performance of optical and acoustic links, by which the maximum bitrate was improved dramatically. To combine the merits of UA and RF links, Soomro *et al.* used UA and RF links for long and close range communication, respectively, which generated high control gains [23]. In [24], Lin *et al.* proposed a software-define networking (SDN)-based WSN for underwater cooperative search by hybrid UL/UA links. However, these works neglected that case that some USNs might be out of the communication range.

Therefore, the flexibility of underwater vehicles (UV) (e.g., AUV) makes it possible to remarkably improve the coverage of underwater data transmission. In [25], an UA-based sensor network aided by AUVs was designed to realize mobile data collection, subject to a system energy constraint. Following [25], Han *et al.* proposed a high-availability scheme to dispatch AUVs to increase the packet delivery ratio [26]. To realize optimal relaying and power control, a reinforcement learning (RL) method was adopted to maximize the signal-to-noise ratio (SNR) of USNs in [27].

Owing to different UCL characteristics, it is worth studying how to jointly select optimal UCLs for data transmission and deploy an energy-efficient UECN. Unfortunately, the existing works [24], [27] and [28] did not synthetically solve the problem mentioned above. In [24], the authors used a hybrid UL/UA network for underwater communication, but did not optimize the link performance (e.g., SNR). In [27], a relay-node selection algorithm was proposed to transfer data to an USV, but this method was only suitable in static scenarios, thus limiting the underwater wireless coverage. To optimize the performance of underwater wireless networks, Xing *et al.* minimized the energy consumption of data transmission and maximized the overall SNR [28], respectively, but indeed this two problems should be optimized simultaneously to obtain the optimal solution. Therefore, we can find that most works just focus on one-layer optimization, i.e., the balance between energy and efficiency is worthy of in-depth discussion. To our best knowledge, this article is one of the first works on joint underwater relay detection and selection, and AUV deployment for underwater emergency communication.

B. Contributions

Motivated by the above, we comprehensively study in this article an UECN aided by multiple UCLs and AUVs to realize energy-efficient underwater emergency response, as shown in Fig. 1. Compared with the previous works in [21]–[28], we consider the practical case that the USNs within the communication range of the USV can forward data to the USV directly, but the rest of USNs disconnect with the USV can transfer data to other USNs or AUVs, namely, relays, by which the data can be finally received by the USV. Here, we aim to simultaneously minimize the amount of time for emergency response and the total energy consumption, and the main contributions are summarized as follows.

- To tackle this new problem, we first define three types of emergency response modes (ERM), denoted by *ERM 1*, *ERM 2*, and *ERM 3*, respectively, and select the optimal ERM for each USN by two steps, including relay detection and selection. Specifically, in the first step, we find out the USNs that can transmit data to the USV directly by greedy searching, and these USNs will work as potential relays to transfer data returned from the rest of USNs. Then, following the distribution of relays, to jointly maximize the channel capacity and ensure the connectivity of UCLs, we use RL-based methods to select the best relay for the USN that disconnects with the USV and find out the USNs that can not connect with the potential relays, namely, the “isolated” USNs (IUSN).

- Next, we need to determine the optimal strategy of AUV deployment so as to better the performance of underwater data transmission, and make sure the collected data returned from IUSNs can be successfully received by the USV. Specifically, we jointly determine the optimal position and control of each AUV by convex optimization, where the UCL channel capacity and AUV velocity are both maximized, so the amount of time spent on underwater data transmission and motion can be shortened. Furthermore, from the perspective of multiobjective optimization problem (MOP), we further obtain the best tradeoff between response efficiency and energy consumption by multiobjective evolution algorithms, subject to a given set of transmit power, signal-to-interference-plus-noise ratio (SINR), outage probability, and system energy constraints

- Finally, numerical results show that our proposed UECN can dramatically enhance emergency response efficiency and effectively manage energy, i.e., the best tradeoff between them is achieved. Especially, by hierarchical segmentation, each USN can work in its optimal ERM, where the optimal UCL and transmit power is jointly optimized. Moreover, with the support of AUVs, we simultaneously minimize the time for emergency response and the energy consumption by solving the optimal number of AUVs and IUSN transmit power. Consequently, the energy-efficient UECN can be established.

C. Organization

The remainder of this article is organized as follows. In Section II, we introduce the system model and the problem formulation. In Section III, we first select the optimal ERMs for USNs and then realize the optimal deployment of AUVs to assist underwater communication. The simulation results and

discussions are presented in Section IV to verify the effectiveness of the proposed approach, and the conclusions are shown in Section V.

Notations: Scalars are denoted by italic letters, and vectors and matrices are denoted by bold-face lower-case and bold-face upper-case letters, respectively. For a real x , $\mathcal{I}(x)$ and $\mathcal{R}(x)$ denote the value of its integral part and remainder, respectively, and $\mathbb{I}(x)$ stands for the indicator function that is equal to 1 if $x > 0$, and 0 otherwise. For a real-valued vector \mathbf{x} , $\|\mathbf{x}\|$ and $\mathbb{E}(\mathbf{x})$ denote its Euclidean norm and expectation, respectively. For a set \mathcal{X} , $|\mathcal{X}|$ denotes its cardinality.

TABLE I
BASIC DIFFERENCES AMONG UCLs

Parameter	UL Links	UA Links	RF Links
Frequency	$10^{12}\text{--}10^{15}$ Hz	10 Hz-100 kHz	MHz ranges
Transmitted power	Few watts	Tens of milliwatts	Few watts
Data rate	Gbps	kbps	Mbps
Communication distance	10-100 m	up to 20 km	up to 10 m
Performance parameter	Absorption, turbulence, and organic matter	Temperature, shipping activity, salinity, and pressure	Conductivity and permeability
Delay	Low	High	Moderate
Propagation speed	2.25×10^8 m/s	1500 m/s	2.25×10^8 m/s
Line-of-Sight (LoS)/None Line-of-Sight (NLoS)	LoS only	Both	Both

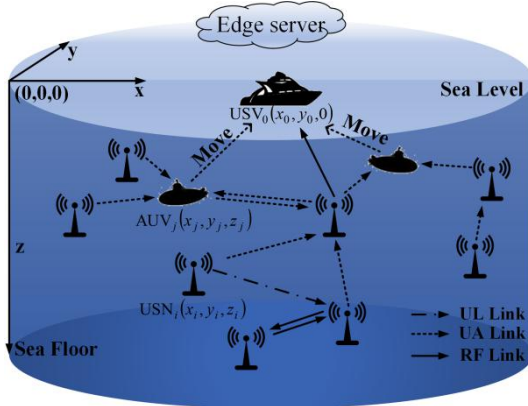


Fig. 1. System model.

II. SYSTEM MODEL AND PROBLEM FORMULATION

A. System Model

The system consists of three units, including $\mathcal{N} = \{1, 2, \dots, N\}$ USNs, $\mathcal{M} = \{1, 2, \dots, M\}$ AUVs, and one USV. In this article, USNs $(x_i^{\text{USN}}, y_i^{\text{USN}}, z_i^{\text{USN}})$, $i \in \mathcal{N}$ are deployed below the sea surface to collect environmental parameters, AUVs $(x_j^{\text{AUV}}, y_j^{\text{AUV}}, z_j^{\text{AUV}})$, $j \in \mathcal{M}$ are dispatched to assist USNs in data transmission, and the USV $(x_0^{\text{USV}}, y_0^{\text{USV}}, 0)$ working as a

gateway does not move on the sea. In our model, we assume that the locations of USNs, AUVs, and an USV are known to a control center (e.g., emergency ship) located at an edge server that is responsible for computation intensive tasks, and three types of UCLs are considered, including UL, UA, and RF links, where the upper bound of transmit power of each UCL are P_{\max}^{UL} , P_{\max}^{UA} , and P_{\max}^{RF} , respectively, and the frequency of each UCL are 10^{13} Hz, 20 kHz, and 5 MHz, respectively. Clearly, in our system, geographically fixed USNs can directly transmit data to the USV if they are close to the USV, or indirectly transfer data to relays, namely, USNs connected with the USV or AUVs. The main aim is to make sure that the data can be finally forwarded to the USV. To this end, we first define the ERM and introduce the path loss (PL) model.

Without loss of generality, three types of ERMs are defined as follows.

- *ERM 1:* The USN directly transmits its data to the USV through the selected UCL.
- *ERM 2:* The USN directly transmits its data to the USNs in *ERM 1* through the selected UCL, and thus the data can be cached and transferred to the USV by a single-hop relay.
- *ERM 3:* The USN directly transmits its data through the selected UCL to an AUV that can move back to the USV to offload data.

Therefore, based on the above three modes, we need to determine the optimal ERM for each USN and make sure that all USNs' emergency data will be received.

Next, to decipher different UCLs, we adopt three types of PL models to reflect the random channel attenuation caused by distance and frequency.

For the UL link, the most commonly used channel is the LoS link (see Table I), where the light beam of the transmitter aligns with the direction of the receiver [12]:

$$L_{i,k}^{\text{UL}}(\text{dB}) = 10 \log_{10} \left(\frac{\eta_T \eta_R \exp[-c(\lambda) d_{i,k}] A_{\text{Rec}}}{2\pi d_{i,k}^2 \cos(\theta)(1 - \cos(\theta_0))} \right) \quad (1)$$

where $d_{i,k}$ is the Euclidean distance between USN i and USN k , η_T and η_R are the optical efficiency of the transmitter and the receiver, respectively, λ is the wavelength, θ is the elevation angle, θ_0 is the laser beam divergence angle, A_{Rec} is the receiver aperture area, and $c(\lambda)$ is given by [29]:

$$c(\lambda) = a(\lambda) + b(\lambda) \quad (2)$$

where $a(\lambda)$ and $b(\lambda)$ are absorption and scattering coefficients, respectively.

For the UA link, the attenuation of UA channels can be expressed as:

$$L_{i,k}^{\text{UA}}(\text{dB}) = \kappa 10 \log_{10} d_{i,k} + \frac{d_{i,k}}{1000} 10 \log_{10} \phi(f) \quad (3)$$

where $\kappa \in [1, 2]$ is the spreading coefficient, f is the frequency, and $10 \log_{10} \phi(f)$ is given by:

$$10 \log_{10} \phi(f) = \frac{0.11 f^2}{1 + f^2} + \frac{44 f^2}{4100 + f^2} + 2.75 \times 10^{-4} f^2 + 0.003 \quad (4)$$

In addition, the ambient noises of UA links can be expressed as follows [16]:

$$\begin{cases} 10\log_{10}N_T(f) = 17 - 30\log_{10}f \\ 10\log_{10}N_S(f) = 40 + 20(s - 0.5) + 26\log_{10}f - 60\log_{10}(f + 0.3) \\ 10\log_{10}N_W(f) = 50 + 7.5\sqrt{w} + 20\log_{10}f - 40\log_{10}(f + 0.4) \\ 10\log_{10}N_{Th}(f) = -15 + 20\log_{10}f \end{cases} \quad (5)$$

where N_T , N_S , N_W , and N_{Th} are the noises derived from turbulence, shipping, waves, and thermal noise, respectively, $s \in [0,1]$ is the shipping factor, w is the wind speed, and the total noise is denoted by $10\log_{10}(N_T(f)N_S(f)N_W(f)N_{Th}(f))$.

For the RF link, the underwater RF PL can be solved by *Maxwell equation* [30]:

$$L_{i,k}^{RF}(\text{dB}) = 8.686\sqrt{\pi\mu f}d_{i,k} \quad (6)$$

where μ is the permeability factor, and ι is the electrical conductivity.

B. Problem Formulation

Given the problem of deploying an energy-efficiency UECN, we can see that the main challenge is to maximize the response efficiency, subject to the energy constraints. In this article, we evaluate the response efficiency by the amount of time for data collection. Since USNs continuously return data and do not move with time, some USNs located far away from the USV must be served by relays. Thus, the response efficiency mainly depends on the time spent on data transmission and AUV movement, and the original problem, denoted by **(OP)**, can be defined as follows:

$$\textbf{(OP)}: \begin{cases} \min & t_j + t_i \approx t_j = (t_R + t_M)_j, j \in \mathcal{M} \\ \min & e_j + e_i \approx e_j = (e_R + e_M)_j, j \in \mathcal{M}, \text{ s.t. } e_j \leq E_{\max} \end{cases} \quad (7)$$

where t_j and e_j denote the amount of time and the energy consumption for AUV j to conduct tasks, respectively, $t_j \gg t_i$, $e_j \gg e_i$, t_i and e_i respectively stand for the time and the energy of USN i to transmit data that can be neglected, t_R and t_M are the time for AUV data transmission and motion, respectively, e_R and e_M are the energy consumed by data transmission and motion, respectively, and E_{\max} is the upper bound of AUV j 's energy.

In (7), t_R depends on $\omega_{i,j}$ and $R_{i,j}$, where $\omega_{i,j}$ is the propagation speed (see Table I), and $R_{i,j}$ denotes the channel capacity defined in [31]:

$$R_{i,j} = B \log_2(1 + \text{SINR}_{i,j}) = B \log_2 \left(1 + \frac{P_{i,j}^{\text{USN}} / 10^{(L_{i,j}^{\text{USN}}/10)}}{N_0 + I} \right) \quad (8)$$

where B is the bandwidth, $P_{i,j}^{\text{USN}}$ is the transmit power, N_0 is the noise power, and I is the variable of interference power.

In addition, t_M depends on AUV motion distance and

velocity. Specifically, according to the kinematics, e_M is defined as [32]:

$$e_M = e_B + e_L + e_S + e_E \quad (9)$$

where e_B , e_L , e_S , and e_E are the energy consumed by the buoyancy system, the linear system, the rotational system, and the electronic system, respectively. First, e_B is given by [33]:

$$e_B = \frac{2m_B}{\eta_B \rho} \left(\mathcal{I} \left(\frac{|z_j^{\text{AUV}}|}{2D_{\max}} \right) \rho g D_{\max} + \rho g \mathcal{R} \left(\frac{|z_j^{\text{AUV}}|}{2D_{\max}} \right) D_{\max} + \mathcal{I} \left(\frac{|z_j^{\text{AUV}}|}{2D_{\max}} \right) P_0 \right) \quad (10)$$

where ρ is the seawater density, η_B is the engine efficiency, m_B is the mass of the net buoyancy, g is the gravity acceleration, D_{\max} is the maximum depth, and P_0 is the atmospheric pressure.

Next, e_L is expressed as:

$$e_L = \left(2\mathcal{I} \left(\frac{|z_j^{\text{AUV}}|}{2D_{\max}} \right) + 1 \right) \frac{m_L a_L^2 (d_{j,0} \cos(\theta))^4}{\eta_L} \quad (11)$$

where m_L is the mass of the movable block, a_L and η_L are the linear system constant and efficiency, respectively, and $d_{j,0}$ is the distance between AUV j and the USV.

To realize the rotation, e_S is represented by:

$$e_S = \frac{1}{2\eta_S} a_S^2 (\psi_1 - \psi_0)^4 \quad (12)$$

where a_S and η_S are the rotational system constant and efficiency, respectively, and ψ_1 and ψ_0 are the final and the initial angle of rotation, respectively.

Finally, to maintain the electronic system, e_E is obtained:

$$e_E = \frac{a_E d_{j,0}}{v_j} \quad (13)$$

where a_E is the electronic system constant, $d_{j,0}$ is the Euclidean distance between AUV j and the USV, and v_j is the velocity.

III. JOINT ERM SELECTION AND AUV DEPLOYMENT

In this section, we first select the optimal ERM for each USN and find out IUSNs, namely, the USN in *ERM 3*, to shorten the time for data transmission by the proposed hierarchical segmentation algorithm. Next, based on the distribution of IUSNs, we dispatch AUVs to collect emergency data returned from IUSNs, where the optimal position and control of each AUV are jointly determined to minimize the amount of time for data collection and motion, respectively. Finally, the best tradeoff between response efficiency and energy consumption is obtained with the help of multiobjective optimization.

A. Optimal ERM Selection

To effectively collect emergency data, we need to determine the optimal ERM for each USN so as to minimize t_R in **(OP)**,

including selection and optimization of UCLs, and to make sure that all USNs' data will be finally forwarded toward the USV, which significantly shortens the amount of time for data transmission and improves the response efficiency. Especially, given the positions of geographically fixed USNs, we can find that the problem of optimal ERM selection can be solved hierarchically, so we solve it by the following two steps.

- *Relay detection*: Given the original distribution of all USNs, we determine the USNs in *ERM 1* that can work as potential relays to transfer data.

- *Relay selection*: Given the distribution of relays, we adopt RL-based methods to find out relays for USNs in *ERM 2* and in *ERM 3*, respectively.

Based on the above two steps, the optimal ERM selection can be realized, where the USNs in *ERM 1* transmit data to the USV directly, the USNs in *ERM 2* transmit data to potential relays, namely, the USNs in *ERM 1*, and the USNs in *ERM 3* must be served by AUVs, as shown in Fig. 2.

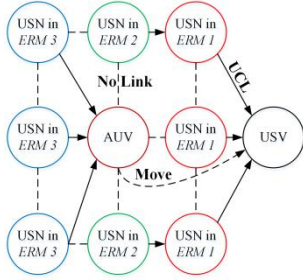


Fig. 2. Optimal ERM selection.

1) Relay Detection

Obviously, we can assert from (OP) and (8) that the optimal ERM selection is equivalent to maximizing $R_{i,0}$, subject to a minimum SINR constraint, denoted by γ , so the objective function can be defined as:

$$\max \sum_{i \in \mathcal{N}} \varphi_i \quad (14)$$

$$\text{s.t. } \varphi_i \in \{0,1\}, i \in \mathcal{N}, \quad (15)$$

$$\gamma \leq \varphi_i \frac{P_{i,0}/10^{(L_{i,0}/10)}}{N_0 + I}, \quad (16)$$

$$P_{i,0} \in \{P_{i,0}^{\text{UL}}, P_{i,0}^{\text{UA}}, P_{i,0}^{\text{RF}}\}, i \in \mathcal{N}, \quad (17)$$

$$L_{i,0} \in \{L_{i,0}^{\text{UL}}, L_{i,0}^{\text{UA}}, L_{i,0}^{\text{RF}}\}, i \in \mathcal{N}, (1), (3), (6), \quad (18)$$

$$0 \leq P_{i,0}^{\text{UL}} \leq P_{\max}^{\text{UL}}, 0 \leq P_{i,0}^{\text{UA}} \leq P_{\max}^{\text{UA}}, 0 \leq P_{i,0}^{\text{RF}} \leq P_{\max}^{\text{RF}} \quad (19)$$

where φ_i is a binary variable that is equal to 1 if USN i can connect with the USV directly; otherwise it is set to 0, N_0 is the noise power, and I is the variable of interference power.

Since (14) is a mixed integer non-linear problem (MINILP) and the constraint of SINR in (16) is non-convex, (14) can not be solved directly. To simplify (14) and make it solvable, we assume that every USN will greedily select the UCL that can maximize its channel capacity for data transmission, so the UCL selection for USN i can be expressed as:

$$L_{i,0} = \underset{\{L_{i,0}^{\text{UL}}, L_{i,0}^{\text{UA}}, L_{i,0}^{\text{RF}}\}}{\operatorname{argmax}} \{R_{i,0}^{\text{UL}}, R_{i,0}^{\text{UA}}, R_{i,0}^{\text{RF}}\} \quad (20)$$

Similarly, the transmit power of USN i is obtained:

$$P_{i,0} = \underset{\{P_{i,0}^{\text{UL}}, P_{i,0}^{\text{UA}}, P_{i,0}^{\text{RF}}\}}{\operatorname{argmax}} \{R_{i,0}^{\text{UL}}, R_{i,0}^{\text{UA}}, R_{i,0}^{\text{RF}}\} \quad (21)$$

Proposition 1: The optimal transmit power of USN i equals $P_{\min} 10^{(L_{i,0}/10)}$, where P_{\min} is threshold of received power.

Proof: Based on (17)-(19), to maximize $R_{i,0}$, the optimal $R_{i,0}^*$ is obtained when only USN i transmits its data to the USV and the rest of USNs stop data transmission, so the optimal SINR equals SNR, namely, $P_{i,0}/10^{(L_{i,0}/10)}/N_0$. However, if so, it will be unfair to other USNs. From the perspective of USN k ($k \neq i$), USN i can not transmit data with its maximum transmit power so as to obtain the best balance between the self gain (SINR) and the interference to USN k (I). Therefore, given the threshold of received power, denoted by P_{\min} , the optimal transmit power of USN i is equal to $P_{\min} 10^{(L_{i,0}/10)}$, and (17) can be redefined as:

$$P_{i,0} = \underset{\{P_{i,0}^{\text{UL}}, P_{i,0}^{\text{UA}}, P_{i,0}^{\text{RF}}\}}{\operatorname{argmax}} \{R_{i,0} | P_{\min} 10^{(L_{i,0}/10)}\} \quad (22)$$

In addition, considering the fact that each USN has a certain possibility to disconnect with the USV, we express the outage probability of USN i as follows [31]:

$$\mathbb{P}_{i,0} = \mathbb{P}\left(P_{i,0}/10^{(L_{i,0}/10)} \leq P_{\min}\right) = 1 - \mathcal{Q}\left(\frac{P_{\min} - P_{i,0}/10^{(L_{i,0}/10)}}{\sigma^2}\right) \quad (23)$$

where σ^2 is the standard deviation, and $\mathcal{Q}(x)$ is the Q-function:

$$\mathcal{Q}(x) = \int_x^\infty \frac{1}{\sqrt{2\pi}} e^{-y^2/2} dy = -\int_\infty^x \frac{1}{\sqrt{2\pi}} e^{-y^2/2} dy \quad (24)$$

To guarantee the continuity of data transmission, given (16), (23), and the threshold of $\mathbb{P}_{i,0}$, denoted by ε , we reformulate (14) as follows:

$$\sum_{i \in \mathcal{N}} \mathbb{I}(\max\{\varepsilon - \mathbb{P}_{i,0}, 0\}) \mathbb{I}\left(\max\left\{\frac{P_{i,0}/10^{(L_{i,0}/10)}}{N_0 + I} - \gamma, 0\right\}\right) \quad (25)$$

$$\text{s.t. } (1), (3), (6), (15) - (19), P_{\min} 10^{(L_{i,0}/10)} \leq P_{i,0}, \quad (26)$$

$$\begin{aligned} I = & \alpha_i^{\text{UL}} \sum_{j \in \mathcal{J}} \mathbb{I}(\max\{\varepsilon - \mathbb{P}_{j,0}^{\text{UL}}, 0\}) P_{j,0}^{\text{UL}} / 10^{(L_{j,0}^{\text{UL}}/10)} \\ & + \alpha_i^{\text{UA}} \sum_{k \in \mathcal{K}} \mathbb{I}(\max\{\varepsilon - \mathbb{P}_{k,0}^{\text{UA}}, 0\}) P_{k,0}^{\text{UA}} / 10^{(L_{k,0}^{\text{UA}}/10)} \\ & + \alpha_i^{\text{RF}} \sum_{l \in \mathcal{L}} \mathbb{I}(\max\{\varepsilon - \mathbb{P}_{l,0}^{\text{RF}}, 0\}) P_{l,0}^{\text{RF}} / 10^{(L_{l,0}^{\text{RF}}/10)}, \end{aligned} \quad (27)$$

$$\alpha_i^{\text{UL}}, \alpha_i^{\text{UA}}, \alpha_i^{\text{RF}} \in \{0,1\}, \alpha_i^{\text{UL}} + \alpha_i^{\text{UA}} + \alpha_i^{\text{RF}} = 1, \quad (28)$$

$$|\mathcal{J}| + |\mathcal{K}| + |\mathcal{L}| = |\mathcal{N}|, \mathcal{J} \cap \mathcal{K} \cap \mathcal{L} = \emptyset \quad (29)$$

where \mathcal{J} , \mathcal{K} , and \mathcal{L} are the set of USNs selecting UL, UA, and RF links, respectively, and $\alpha_i^{\text{UL}} + \alpha_i^{\text{UA}} + \alpha_i^{\text{RF}} = 1$ ensures that just one type of UCLs is selected by each USN.

Following (14)-(24), (25) can be solved by traversing all USNs in \mathcal{N} . As a result, we can obtain the set of USNs in *ERM 1*, denoted by \mathcal{A} , as shown in Algorithm 1. Moreover, the set of the rest of USNs can be denoted by $\mathcal{N} \setminus \mathcal{A}$. Clearly, the USNs in \mathcal{A} will further work as relays to transfer the data returned from the USNs in *ERM 2*. The computational complexity of Algorithm 1 depends on step 4-13, denoted by $\mathcal{O}(|\mathcal{N}||\mathcal{N} \setminus \mathcal{A}|)$.

Algorithm 1 Algorithm for Determining USNs in *ERM 1*

```

1: Input: Set of USNs  $\mathcal{N}$ 
2: Output: Set of USNs in ERM 1
3: Initialize:  $\mathcal{A} = \emptyset$ 
4: for  $i \in \mathcal{N}$  do
5:   Compute  $L_{i,0}$ ,  $P_{i,0}$ , and  $\mathbb{P}_{i,0}$  by (20), (22), and (23),
   respectively
6:   Determine  $\alpha_i^{\text{UL}}, \alpha_i^{\text{UA}}$ , and  $\alpha_i^{\text{RF}}$  based on the type of
   USN  $i$ 's UCL
7:   for  $j \in \mathcal{N} \setminus i$  do
8:     Let  $R_{j,0} = \max \{R_{j,0}^{\text{UL}}, R_{j,0}^{\text{UA}}, R_{j,0}^{\text{RF}}\}$ , and select the
   optimal UCL for USN  $j$ 
9:   end for
10:  if  $\mathbb{I}(\max \{\mathcal{E} - \mathbb{P}_{i,0}, 0\}) \mathbb{I}\left(\max \left\{\frac{P_{i,0}/10^{(L_{i,0}/10)}}{N_0 + I} - \gamma, 0\right\}\right) = 1$ 
then
11:    Add  $i$  to  $\mathcal{A}$ 
12:  end if
13: end for
14: return  $\mathcal{A}$ 

```

2) Relay Selection

In this section, based on \mathcal{A} and $\mathcal{N} \setminus \mathcal{A}$, we further divide $\mathcal{N} \setminus \mathcal{A}$ into two sets, namely, the set of USNs in *ERM 2* and the set of USNs in *ERM 3*, denoted by \mathcal{B} and \mathcal{C} , respectively. Specifically, the USN in \mathcal{B} will select one USN in \mathcal{A} as its relay, and the USN in \mathcal{C} will be served by AUVs.

As mentioned in (OP), owing to $t_j \gg t_i$, we can assert that our target is to maximize the number of USNs in *ERM 2* as many as possible, i.e., let $\mathcal{C} = \emptyset$ so as to reduce the number of USNs served by AUVs, thus reducing the time for emergency response, so the objective function is defined as follows:

$$\max \sum_{i \in \mathcal{N} \setminus \mathcal{A}} \sum_{k \in \mathcal{A}} \beta_k \mathbb{I}(\max \{\mathcal{E} - \mathbb{P}_{i,k}, 0\}) \mathbb{I}(\max \{R_{i,k} - \bar{R}, 0\}) \quad (30)$$

$$\text{s.t. } \beta_k \in \{0, 1\}, \sum_{k \in \mathcal{A}} \beta_k = 1 \quad (31)$$

where \bar{R} is equal to $\frac{1}{|\mathcal{A}|} (R_{i,1} + \dots + R_{i,|\mathcal{A}|})$, and $\sum_{k \in \mathcal{A}} \beta_k = 1$ ensures that just one USN relay is selected by each USN.

To solve (30), we aim to find a policy that can 1) maximize the number of USNs in \mathcal{B} 2) maximize the channel capacity $R_{i,k}$ and 3) ensure the connectivity between USNs and relays. However, it is challenging to obtain the best balance between

these objectives, because (30) and (31) are both non-convex and some traditional algorithms (e.g., *Dijkstra algorithm* [34]) are too time-consuming. Fortunately, with the help of RL, the optimal strategy for selection problems can be found out, because RL-based methods (e.g., Q-learning, deep Q-network (DQN) [35], etc) can heuristically search possible solutions from the system action space and effectively learn experiences from the system feedback. Therefore, before finding the optimal relays for USNs, we first define the system state, action, and reward of RL, respectively, as follows.

• *State*: The set of states, denoted by \mathbf{s}_t (at each time slot t), is defined as:

$$\mathbf{s}_t = [\mathbb{P}_{i,k}^{\text{UL}}, \mathbb{P}_{i,k}^{\text{UA}}, \mathbb{P}_{i,k}^{\text{RF}}, R_{i,k}^{\text{UL}}, R_{i,k}^{\text{UA}}, R_{i,k}^{\text{RF}}] i \in \mathcal{N} \setminus \mathcal{A}, k \in \mathcal{A} \quad (32)$$

where USN i in $\mathcal{N} \setminus \mathcal{A}$ only selects one USN relay k in \mathcal{A} through the optimal UCL, which will be observed at each time slot.

• *Action*: The set of actions, denoted by \mathbf{a}_t (at each time slot t), is defined as:

$$\mathbf{a}_t = [1, 2, \dots, |\mathcal{A}| - 1, |\mathcal{A}|] \quad (33)$$

where $|\mathcal{A}|$ is the index of relays. USN i will select one potential relay in \mathcal{A} at each time slot, and each relay can be repeatedly selected by different USNs.

• *Reward*: The reward, denoted by r_t (at each time slot t), is given by:

$$r_t = \max \left\{ \begin{aligned} &\mathbb{I}(\max \{\mathcal{E} - \mathbb{P}_{i,k}^{\text{UL}}, 0\}) R_{i,k}^{\text{UL}}, \\ &\mathbb{I}(\max \{\mathcal{E} - \mathbb{P}_{i,k}^{\text{UA}}, 0\}) R_{i,k}^{\text{UA}}, \\ &\mathbb{I}(\max \{\mathcal{E} - \mathbb{P}_{i,k}^{\text{RF}}, 0\}) R_{i,k}^{\text{RF}} \end{aligned} \right\}, i \in \mathcal{N} \setminus \mathcal{A}, k \in \mathcal{A} \quad (34)$$

where USN i will select optimal UCL to maximize its channel capacity.

Next, based on (32)-(34), we need to train an optimal strategy for selecting the relay of each USN at each time slot t , i.e., each USN selects an action, denoted by $a \in \mathbf{a}_t$, according to the current policy, denoted by π , and generates a reward r_t based on the action feedback. Further, each USN will continuously update the policy π until find the best policy π^* to maximize its reward [27], as shown in Algorithm 2:

$$\begin{aligned} Q(a_t, \mathbf{s}_t) &= Q(a_t, \mathbf{s}_t) + \alpha \left(r_t + \beta \max_{a \in \mathbf{a}_{t+1}} \{Q(a, \mathbf{s}_{t+1})\} - Q(a_t, \mathbf{s}_t) \right) \\ &= (1 - \alpha) Q(a_t, \mathbf{s}_t) + \alpha \left(r_t + \beta \max_{a \in \mathbf{a}_{t+1}} \{Q(a, \mathbf{s}_{t+1})\} \right) \end{aligned} \quad (35)$$

where $Q(a_t, \mathbf{s}_t)$ is the value of the Q-table that records the system actions and states, α is the learning rate, β is the discount factor, and \mathbf{s}_{t+1} is the next state from the current state \mathbf{s}_t via the selected action a . To avoid the local maximum [36], we use ℓ -greedy algorithm to select an action $a = \arg \max_{a \in \mathbf{a}_t} \{Q(a, \mathbf{s}_t)\}$ with a probability $1 - \ell$, where ℓ is a relatively small probability:

$$\pi \leftarrow \begin{cases} 1-\ell & a = \arg\max_{a \in \mathbf{a}_t} \{Q(a, \mathbf{s}_t)\} \\ \ell & a \neq \arg\max_{a \in \mathbf{a}_t} \{Q(a, \mathbf{s}_t)\} \end{cases} \quad (36)$$

Similar to Q-learning, Sarsa-based method [37] also uses Q-table to record its actions and states, but the Q-value of Sarsa is updated by $Q(\mathbf{a}_{t+1}, \mathbf{s}_{t+1})$ rather than $\arg\max_{a \in \mathbf{a}_{t+1}} \{Q(a, \mathbf{s}_{t+1})\}$.

Compared with the efficiency of Q-table in (35), DQN uses a convolutional neural network (CNN) including 2 convolutional layers and 2 fully connected layers to estimate the Q-value, as shown in Algorithm 3, and adopts the memory replay to deal with the problem of high dimensions. Thus, the loss function of DQN is given by [38]:

$$f(\mathbf{w}_t) = \mathbb{E} \left[\left(r_t + \beta \max_{a \in \mathbf{a}_{t+1}} \{Q(a, \mathbf{s}_{t+1}, \mathbf{w}_t)\} - Q(a_t, \mathbf{s}_t, \mathbf{w}_t) \right)^2 \right] \quad (37)$$

where \mathbf{w}_t is the vector of neuron parameters (weights) that can be optimized by stochastic gradient descent (SGD), and

$$\frac{\partial f(\mathbf{w}_t)}{\partial \mathbf{w}_t} = -\mathbb{E} \left[\left(r_t + \beta \max_{a \in \mathbf{a}_{t+1}} \{Q(a, \mathbf{s}_{t+1}, \mathbf{w}_t)\} - Q(a_t, \mathbf{s}_t, \mathbf{w}_t) \right) \frac{\partial Q(a_t, \mathbf{s}_t, \mathbf{w}_t)}{\partial \mathbf{w}_t} \right].$$

Based on Algorithm 2 and Algorithm 3, we can obtain the optimal $R_{i,k}^*$ of USN i by comparing the results derived from Algorithm 2 and Algorithm 3, respectively, and thus (30) can be solved to obtain \mathcal{B} and \mathcal{C} , as shown in Algorithm 4. By the proposed hierarchical segmentation, the optimal ERM selection can be finally realized.

Algorithm 2 Algorithm for Q-table-based Relay Selection

- 1: **Input:** Set of relays \mathcal{A}
 - 2: **Output:** Optimal relay of USN $i, i \in \mathcal{N} \setminus \mathcal{A}$
 - 3: **Initialize:** Number of episode L and number of epoch T
 - 4: **for** $l = 1, \dots, L$, **do**
 - 5: **for** $t = 1, \dots, T$, **do**
 - 6: Compute $\mathbf{s}_t = [\mathbb{P}_{i,k}^{\text{UL}}, \mathbb{P}_{i,k}^{\text{UA}}, \mathbb{P}_{i,k}^{\text{RF}}, R_{i,k}^{\text{UL}}, R_{i,k}^{\text{UA}}, R_{i,k}^{\text{RF}}]$ based on (8) and (23)-(24)
 - 7: Select action a based on (36)
 - 8: Compute \mathbf{s}_{t+1} and r_t based on (32) and (34)
 - 9: Update $Q(a_t, \mathbf{s}_t)$ based on (35)
 - 10: $\mathbf{s}_t \leftarrow \mathbf{s}_{t+1}$
 - 11: **end for**
 - 12: **end for**
 - 13: return USN i 's relay with the maximum $R_{i,k}^*$
-

Algorithm 3 Algorithm for DQN-based Relay Selection

- 1: **Input:** Set of relays \mathcal{A}
- 2: **Output:** Optimal relay of USN $i, i \in \mathcal{N} \setminus \mathcal{A}$
- 3: **Initialize:** Number of episode L , number of epoch T , number of features N , number of training M , and $\mathcal{D} = \emptyset$
- 4: **for** $l = 1, \dots, L$, **do**
- 5: **for** $t = 1, \dots, T$, **do**
- 6: Compute $\mathbf{s}_t = [\mathbb{P}_{i,k}^{\text{UL}}, \mathbb{P}_{i,k}^{\text{UA}}, \mathbb{P}_{i,k}^{\text{RF}}, R_{i,k}^{\text{UL}}, R_{i,k}^{\text{UA}}, R_{i,k}^{\text{RF}}]$ based on (8) and (23)-(24)

- 7: Input $\phi_t = [\mathbf{s}_t, \dots, \mathbf{s}_{t-N}]$ to the CNN
 - 8: Select action a based on (36)
 - 9: Compute \mathbf{s}_{t+1} and r_t based on (32) and (34)
 - 10: $\mathcal{D} \leftarrow \mathcal{D} \cup \{\mathbf{s}_t, a_t, r_t, \mathbf{s}_{t+1}\}$
 - 11: **for** $m = 1, \dots, M$ **do**
 - 12: Select $\{\mathbf{s}_m, a_m, r_m, \mathbf{s}_{m+1}\}$ from \mathcal{D} randomly
 - 13: Compute $r_m + \beta \max_{a \in \mathbf{a}_{m+1}} \{Q(a, \mathbf{s}_{m+1}, \mathbf{w}_m)\}$
 - 14: **end for**
 - 15: Update \mathbf{w}_t based on $\nabla_{\mathbf{w}_t} L(\mathbf{w}_t)$ and SGD
 - 16: **end for**
 - 17: **end for**
 - 18: return USN i 's relay with the maximum $R_{i,k}^*$
-

Algorithm 4 Algorithm for Optimal ERM Selection

- 1: **Input:** Set of USNs \mathcal{N}
 - 2: **Output:** Sets of USNs in $ERM 1$, $ERM 2$, and $ERM 3$, respectively
 - 3: **Initialize:** $\mathcal{A} = \emptyset$, $\mathcal{B} = \emptyset$, and $\mathcal{C} = \emptyset$
 - 4: Update \mathcal{A} based on Algorithm 1
 - 5: **for** $i \in \mathcal{N} \setminus \mathcal{A}$ **do**
 - 6: Determine the relay k of USN i by $\arg\max_k \{R_{i,x}, R_{i,y}\}, x, y \in \mathcal{A}$ derived from Algorithm 2 and Algorithm 3, respectively
 - 7: **if** $\mathbb{I}(\max\{\mathcal{E} - \mathbb{P}_{i,k}, 0\}) \mathbb{I}(\max\{R_{i,k} - \bar{R}, 0\}) = 1$ **then**
 - 8: Add k to \mathcal{B}
 - 9: **end if**
 - 10: **end for**
 - 11: Let $\mathcal{C} = \mathcal{N} \setminus \mathcal{A} \setminus \mathcal{B}$
 - 12: return \mathcal{A} , \mathcal{B} , and \mathcal{C}
-

The computational complexity of Algorithm 2 equals to $\mathcal{O}(LT)$, where L and T are the numbers of episode and epoch, respectively. Similarly, the computational complexity of Algorithm 3 is denoted by $\mathcal{O}(LTM)$, where M is the number of training. For Algorithm 4, it can be regarded as the integration of Algorithm 1-3, so its computational complexity depends on step 4-10, denoted by $\max\{\mathcal{O}(|\mathcal{N}| |\mathcal{N} \setminus \mathcal{A}|), \mathcal{O}(|\mathcal{N} \setminus \mathcal{A}| LTM)\}$.

B. Optimal AUV Deployment

Based on Algorithm 4, IUSNs located far away from the sea surface are found out, i.e., USNs in \mathcal{C} can not transmit data to the USV or USN relays, so they must be served by AUVs. Therefore, AUVs can assist IUSNs in underwater data collection. To this end, we determine the optimal position and control of each AUV to shorten the amount of time for data collection and underwater motion, respectively.

From (OP), we can find that the response efficiency of AUV-aided underwater communication depends on two parts, including t_R and t_M . Specifically, the expressions of t_R and t_M can be respectively defined as follows:

$$(t_R)_j = \frac{p_{i,j}}{R_{i,j}} + \frac{d_{i,j}}{\omega_{i,j}}, i \in \mathcal{C}, j \in \mathcal{M} \quad (38)$$

where $d_{i,j} = \sqrt{(x_j^{\text{AUV}} - x_i^{\text{USN}})^2 + (y_j^{\text{AUV}} - y_i^{\text{USN}})^2 + h_{i,j}^2}$ is the distance between USN i and AUV j , $h_{i,j} = z_j^{\text{AUV}} - z_i^{\text{USN}}$, $p_{i,j}$ is the packet size, and $\omega_{i,j}$ is the propagation speed.

$$(t_M)_j = \frac{d_{j,0}}{v_j}, j \in \mathcal{M} \quad (39)$$

where $d_{j,0} = \sqrt{(x_j^{\text{AUV}} - x_0^{\text{USV}})^2 + (y_j^{\text{AUV}} - y_0^{\text{USV}})^2 + (z_j^{\text{AUV}})^2}$, and v_j is the velocity of AUV j . Thus, we first need to determine the optimal $R_{i,j}$ and $d_{i,j}$ in (38), and then (39) can be optimized by solving optimal $d_{j,0}$ and v_j based on the result of (38).

Proposition 2: Optimizing (38) is equivalent to minimizing $d_{i,j}$.

Proof: Given (8), (22), and (27)-(29), we first define the objective function of (38) as follows:

$$\min (t_R)_j = \frac{p_{i,j}}{B \log_2 \left(1 + \frac{P_{i,j}/10^{(L_{i,j}/10)}}{N_0 + I} \right)} + \frac{d_{i,j}}{\omega_{i,j}} \quad (40)$$

$$\text{s.t. } i \in \mathcal{C}, j \in \mathcal{M}, (18), (27) - (29) \quad (41)$$

Next, we regard $d_{i,j}$ as an independent variable in $L_{i,j}$ and obtain the first derivative of $L_{i,j}^{\text{UL}}$, $L_{i,j}^{\text{UA}}$, and $L_{i,j}^{\text{RF}}$, respectively, as follows:

$$\frac{dL_{i,j}^{\text{UL}}}{dd_{i,j}} = \frac{-10(c(\lambda)d_{i,j} + 2)}{\ln 10(d_{i,j})} < 0 \quad (42)$$

$$\frac{dL_{i,j}^{\text{UA}}}{dd_{i,j}} = \frac{\kappa 10}{\ln 10 d_{i,j}} + \frac{10 \log_{10} \phi(f)}{1000} > 0 \quad (43)$$

$$\frac{dL_{i,j}^{\text{RF}}}{dd_{i,j}} = 8.686 \sqrt{\pi \mu f} > 0 \quad (44)$$

Since (43) and (44) are both greater than 0, it is easy to directly optimize $L_{i,j}^{\text{UA}}$ and $L_{i,j}^{\text{RF}}$ by minimizing $d_{i,j}$. However, from (42), we can find that the monotonicity of $L_{i,j}^{\text{UL}}$ is different from $L_{i,j}^{\text{UA}}$ and $L_{i,j}^{\text{RF}}$. Hence, considering the case that the minimum of $L_{i,j}^{\text{UL}}$ can be obtained when AUV j aligns with USN i , i.e., $\cos(\theta) \leq \cos(\theta_0)$, we can obtain:

$$10 \log_{10} \left(\frac{\eta_T \eta_R \exp[-c(\lambda)d_{i,j}] A_{\text{Rec}}}{2\pi d_{i,j}^2 (1 - \cos(\theta_0))} \right) \leq L_{i,j}^{\text{UL}} \quad (45)$$

where the equality holds, if and only if θ is equal to 0, namely, $h_{i,j} = 0$. However, once $d_{i,j}$ is maximized in $L_{i,j}^{\text{UL}}$, $d_{k,j}$ ($k \neq i$)

is minimized. Therefore, the optimal $d_{i,j}$ can be solved by traversing all USNs in \mathcal{C} , subject to the UL link constraint (see Table I):

$$\min \sum_{j \in \mathcal{M}} \sum_{i \in \mathcal{C}} \sqrt{(x_j^{\text{AUV}} - x_i^{\text{USN}})^2 + (y_j^{\text{AUV}} - y_i^{\text{USN}})^2} \quad (46)$$

Finally, following (46), we can know that when $h_{i,j} = 0$, $L_{i,j}^{\text{UL}}$ can be minimized by minimizing $d_{i,j}$. Clearly, (40)-(46) prove the proposition.

Given the proposition 2, we can further determine the optimal position of AUV j so as to minimize (38), and the objective function of (38) is given by:

$$\min \sum_{j \in \mathcal{M}} \sum_{i \in \mathcal{C}} (t_R)_j = \frac{p_{i,j}}{R_{i,j}} + \frac{d_{i,j}}{\omega_{i,j}} \quad (47)$$

Clearly, it is obvious that minimizing $d_{i,j}$ can yield the maximum of $d_{k,j}$. Therefore, to effectively solve (47), some clustering algorithms (e.g., *K-means clustering* (KMC) [39] and *mean shift clustering* (MSC) [40]) can be used to determine the optimal position of AUV j . In this article, we use KMC to solve (47), and further propose an adaptive KMC (AKMC) to optimize the input of KMC, namely, the number of AUVs (see next section), and it is notable that the number of AUVs and the initial positions of AUVs must be given in advance, and traditional KMC mainly includes steps:

Step 1: Initialize K centroids.
Step 2: Allocate each node to its closest centroid, and generate K clusters.
Step 3: Recompute the centroid of each cluster.
Step 4: Repeat **Step 2** and **Step 3** until clusters do not change.

Similarly, to effectively save the time for underwater motion (t_M), we need to jointly optimize $d_{j,0}$ and v_j for AUV j , subject to the energy constraints (9)-(13). Based on (47), we can define the objective function of $d_{j,0}$ as follows:

$$\min \sum_{j \in \mathcal{M}} \sum_{i \in \mathcal{C}} d_{i,j} + \sum_{j \in \mathcal{M}} d_{j,0} \quad (48)$$

Here, (48) can be also solved by KMC. To utilize the result of (47), we set the initial positions of AUVs as

$$\left\{ x_j^{\text{AUV}}, y_j^{\text{AUV}}, z_j^{\text{AUV}} \right\} \underset{\{x_j^{\text{AUV}}, y_j^{\text{AUV}}, z_j^{\text{AUV}}\}}{\text{argmin}} \sum_{j \in \mathcal{M}} \sum_{i \in \mathcal{C}} (t_R)_j = \frac{p_{i,j}}{R_{i,j}} + \frac{d_{i,j}}{\omega_{i,j}} \text{ derived from (47)}$$

rather than random initialization, which can speed up the convergence of KMC.

Proposition 3: The optimal v_j is given by:

$$v_j^* = \min \left\{ \frac{a_E d_{j,0}}{E_{\text{max}} - (e_R + e_B + e_L + e_S)_j}, v_{\text{max}} \right\} \quad (49)$$

where v_{max} is the maximum velocity of AUV j .

Proof: From the perspective of cost-efficient control, we need to solve the minimum of t_M , i.e., yields the maximum speed, subject to the energy constraint, so the objective function is given by:

$$\max v_j \quad (50)$$

$$\text{s.t. } (e_R + e_M)_j \leq E_{\max}, v_j \leq v_{\max} \quad (51)$$

Next, we derive the Lagrangian cost function of (50):

$$L(v_j, \mathcal{G}_1, \mathcal{G}_2) = v_j + \mathcal{G}_1 \left((e_R + e_B + e_L + e_S)_j + \frac{a_E d_{j,0}}{v_j} - E_{\max} \right) + \mathcal{G}_2 (v_j - v_{\max}) \quad (52)$$

where $\mathcal{G}_1 \geq 0$ and $\mathcal{G}_2 \geq 0$ are the Lagrangian multipliers, and the Karush-Kuhn-Tucker (KKT) conditions are given by:

$$\nabla_{v_j} L(v_j, \mathcal{G}_1, \mathcal{G}_2) = 1 + \mathcal{G}_1 \left(-\frac{a_E d_{j,0}}{v_j^2} \right) + \mathcal{G}_2 = 0, \quad (53)$$

$$\mathcal{G}_1 \left((e_R + e_B + e_L + e_S)_j + \frac{a_E d_{j,0}}{v_j} - E_{\max} \right) = 0, \quad (54)$$

$$\mathcal{G}_2 (v_j - v_{\max}) = 0, \quad (55)$$

$$(e_R + e_B + e_L + e_S + e_E)_j - E_{\max} \leq 0, \quad (56)$$

$$v_j - v_{\max} \leq 0, \quad (57)$$

Therefore, by solving (53)-(57), we can obtain the optimal v_j , and the Lagrangian multiplier \mathcal{G}_1 and \mathcal{G}_2 , which clearly proves the proposition.

Given (47)-(49), we can determine the optimal position and control of each AUV, thus reducing the amount of time for emergency response.

C. Optimal Solution of OP

Following the framework proposed in [41], we adopt multiobjective optimization to jointly determine the optimal number of AUVs and the optimal transmit power of IUSNs so as to achieving the best tradeoff between response efficiency and energy consumption.

Generally, a MOP is given by [41]:

$$\max F(\mathbf{x}) = (f_1(\mathbf{x}), \dots, f_m(\mathbf{x})) \quad (58)$$

$$\text{s.t. } \mathbf{x} \in \Omega \quad (59)$$

where Ω is the variable space, and m is the number of objective functions. As illustrated in [41], we can see that no \mathbf{x} can maximize all objective functions simultaneously, so a best tradeoff from the PF must be found out to balance them. It is well known that approximation of the PF can be decomposed into many scalar subproblems. Motivated by this basic idea, we adopt the *Tchebycheff approach* (TA) [42] to determine the best tradeoff of (7).

Following (47)-(51), we can find that the approximation of (OP) depends on the number of AUVs and the transmit power of IUSNs. It is impossible to minimize the amount of time for data collection and the energy consumption simultaneously, i.e., increasing the number of AUVs saves the amount of time for emergency response, but increases the energy consumption, so it is necessary to find the best tradeoff between them. Since AUVs works simultaneously, optimizing t_j is equivalent to a

minimization-maximization problem (MMP), i.e., the amount of time for emergency response depends on the longest working time of AUVs, but optimizing e_j is equivalent to minimizing the cumulative sum of e_j , i.e., the total energy consumption depends on all AUVs, which is just a minimization problem. Therefore, we can first redefine (OP) as follows:

$$\min \max \{t_j\}, j \in \mathcal{M} \quad (60)$$

$$\min \sum_{j \in \mathcal{M}} e_j \quad (61)$$

Next, owing to merits of KMC, the number of cluster-heads must be given in advance, so (60)-(61) can be formulated as the following MOP, subject to a given set of constraints:

$$\min f_1 = \max \{t_j(x_1, x_2)\} \quad (62)$$

$$\min f_2 = \sum_{j \in \mathcal{M}} e_j(x_1, x_2) \quad (63)$$

$$\text{s.t. } g_1 = x_2 - P_{\min} 10^{(L_{i,j}/10)} \geq 0, i \in \mathcal{C}, (20)-(22), \quad (64)$$

$$g_2 = E_{\max} - e_j(x_1, x_2) \geq 0, \quad (65)$$

$$1 \leq x_1 \leq |\mathcal{C}|, \quad (66)$$

$$0 \leq x_2 \leq P_{\max}, (19), \quad (67)$$

$$(9)-(13), (38)-(39) \quad (68)$$

where x_1 denotes the number of AUVs that is the input of KMC, x_2 denotes the transmit power of IUSNs, and $x_1 \leq |\mathcal{C}|$ means that the number of AUVs can not exceed the number of IUSNs. Here, given the threshold that each AUV can serve, denoted by N_{\max} , we let $x_1 = x_1 + 1$ if the number of IUSNs served by AUVs exceeds N_{\max} . Then, (62)-(63) are simplified as follows by TA:

$$\max g^{\text{TA}}(\mathbf{x}|\boldsymbol{\lambda}, \mathbf{z}^*) = \min_{1 \leq i \leq 2} \{\lambda_i |f_i(\mathbf{x}) - z_i^*\} \quad (69)$$

where $\mathbf{x} = (x_1, x_2)$, $\mathbf{z}^* = (z_1^*, z_2^*)$ is the reference vector minimizing $F(\mathbf{x}) = (f_1(\mathbf{x}), f_2(\mathbf{x}))$, $\boldsymbol{\lambda} = (\lambda_1, \lambda_2)$ is the weight vector, and (69) generates the follows during each iteration, as shown in Algorithm 5:

$$\begin{cases} \{\mathbf{x}^1, \dots, \mathbf{x}^i\}, \\ \text{FV}^i = F(\mathbf{x}^i), \\ \mathbf{z}_i^*, \\ \mathcal{E} = \{\text{FV}^i\} \end{cases} \quad (70)$$

where \mathbf{x}^i is the current solution of objective function i , FV is the function value vector, z_i^* is the best value of the objective function i , and \mathcal{E} is the external population for non-dominated solutions.

Based on \mathcal{E} derived from Algorithm 4, we need to find out the best tradeoff point from the PF. Here, the weight-based method is used to determine the Pareto Optimality (PO), and the weight of objective function i is given by [43]:

$$w_i = \frac{(\max \{f_i\} - f_i) / (\max \{f_i\} - \min \{f_i\})}{\sum_i (\max \{f_i\} - f_i) / (\max \{f_i\} - \min \{f_i\})} \quad (71)$$

Finally, by solving (60)-(61), the optimal number of AUVs and the optimal transmit power of IUSNs are jointly solved, i.e., simultaneously minimize the amount of time for emergency response and the energy consumption, so the energy efficiency can be improved correspondingly.

Algorithm 5 Algorithm for Finding PF

```

1: Input: MOP (62)-(63), Number of Subproblems  $M$ ,
Population Size  $N$ , Weight Vector  $\{\lambda^1, \dots, \lambda^N\}$ , Number of
Neighbourhood Weight Vectors  $T$ , and Threshold  $N_{\max}$ 
2: Output:  $\{FV^1, \dots, FV^N\}$ 
3: Initialize:  $\{i_1, \dots, i_{T_j}\}, i = 1, \dots, N$ ,  $\{\lambda^{i_1}, \dots, \lambda^{i_T}\}$ ,  $\{\mathbf{x}^1, \dots, \mathbf{x}^N\}$ ,
 $\{z_1^*, \dots, z_M^*\}$ , Flag  $F = 1$ , and  $\mathcal{E} = \emptyset$ 
4: for  $i = 1, 2, \dots, N$  do
5:   Select  $m$  and  $n$  from  $\{i_1, \dots, i_{T_j}\}$  and generate  $\mathbf{x}'$  based on
 $\mathbf{x}^m$  and  $\mathbf{x}^n$  by genetic operators
6:   Update  $\mathbf{x}''$  based on  $\mathbf{x}'$  by the heuristic
repair/improvement
7:   while  $F = 1$  do
8:     Generate  $x_1$  clusters  $\{C_1, \dots, C_{x_1}\}$  based on KMC
9:     for  $C_c \in \{C_1, \dots, C_{x_1}\}$  do
10:      if  $|C_c| > N_{\max}$  then
11:        Let  $x_1 = x_1 + 1$  and  $F = 1$ , and update  $\mathbf{x}''$ 
12:      break
13:      else
14:         $F = 0$ 
15:      end if
16:    end for
17:  end while
18:  for  $j = 1, 2, \dots, M$  do
19:    if  $z_j^* > f_j(\mathbf{x}'')$  then
20:      Update  $z_j^* = f_j(\mathbf{x}'')$  based on (62)-(68)
21:    end if
22:  end for
23:  for  $k = 1, 2, \dots, \{i_1, \dots, i_{T_j}\}$  do
24:    if  $g^{\text{TM}}(\mathbf{x}'' | \lambda^k, z^*) \leq g^{\text{TM}}(\mathbf{x}'' | \lambda^k, z^*)$  then
25:       $\mathbf{x}^k = \mathbf{x}''$  and  $FV^k = F(\mathbf{x}'')$ 
26:    end if
27:  end for
28:  Remove all vectors dominated by  $F(\mathbf{x}'')$  from  $\mathcal{E}$ 
29:  Add  $F(\mathbf{x}'')$  to  $\mathcal{E}$  when no vector in  $\mathcal{E}$  dominates  $F(\mathbf{x}'')$ 
30: end for
31: return  $\mathcal{E}$ 

```

In Algorithm 5, we can find that $C_c \in \{C_1, \dots, C_{x_1}\}$ changes dynamically, so the maximum of computational complexity can be denoted by $\mathcal{O}(NMT|C_c|)$.

IV. SIMULATION RESULTS AND DISCUSSIONS

In our simulations, we randomly deploy USNs on a 500×500 m geographic area, where the maximum depth equals 200 m, and the number of USNs is equal to 100, and the simulation parameters are listed in Table II. To verify the effectiveness of our approach, we compare our approach with the benchmark approach proposed in [44]. In [44], the authors used the Kuhn-Munkres algorithm (KMA) [45] to assign relays for multiple users over wireless optical channels, but did not take into account the merits of multiple UCLs and AUVs. By contrast, we first propose a hierarchical segmentation algorithm to select the optimal ERM for each USN with the help of greedy searching and RL, subject to a given set of transmit power, SINR, and outage probability constraints. Next, we optimize the position and velocity of each AUV to assist underwater communication, and the best tradeoff between response efficiency and energy consumption is achieved by jointly solving the optimal number of AUVs and the optimal transmit power of IUSNs, i.e., minimize the amount of time and the energy consumption of emergency response simultaneously. It is worth noting that all simulation results are averaged over a large number of experiments through Python, including NUMPY, CVXPY, GYM, PYMOO, etc.

TABLE II
SIMULATION PARAMETERS

Parameter	Description	Value
η_T	Optical efficiency of the transmitter	0.9
η_R	Optical efficiency of the receiver	0.9
$c(\lambda)$	Extinction coefficient	0.1514
A_{Rec}	Receiver aperture area	0.01 m^2
θ_0	Laser beam divergence angle	68.0°
κ	Spreading coefficient	1.5
s	Shipping factor	0.5
w	Wind speed	0.5 m/s
μ	Permeability factor	$1.256 \times 10^{-6} \text{ H/m}$
t	Electrical conductivity	0.01 S/m
N_0	Noise power	-130.0 dBm
P_{\max}^{UL}	Maximum UL transmit power	10.0 mW
P_{\max}^{UA}	Maximum UA transmit power	5.0 W
P_{\max}^{RF}	Maximum RF transmit power	5.0 W
ρ	Seawater density	1027.0 kg/m^3
η_B	Engine efficiency	0.7
m_B	Mass of the net buoyancy	0.494 kg
g	Gravity acceleration	9.8 m/s^2
D_{\max}	Maximum depth	200.0 m
P_0	Atmospheric pressure	101.325 kPa
m_L	Mass of the movable block	11.0 kg
a_L	Linear system constant	0.1
η_L	Linear system efficiency	0.85
a_S	Rotational system constant	1.0
η_S	Rotational system efficiency	0.85
a_E	Electronic system constant	1.5

ε	Threshold of outage probability	0.01
P_{\min}	Threshold of received power	5.0 dB
p	Packet size	1 Mb
v_{\max}	Maximum velocity	1.0 m/s

In Fig. 3, we present the results of optimal ERM selection derived from Algorithm 4. Fig. 3(a) illustrates the distribution of relays under the sea level, where the USNs in *ERM 2* will select potential relays (USNs in *ERM 1*) to transfer its data. As illustrated in Fig. 3(b), the USNs in *ERM 3* will be served by AUVs. As a result, each USN works in its optimal ERM and transmits the collected emergency data toward the USV directly or indirectly through the optimal UCL, i.e., by solving (14) and (30), we can obtain 1) the distribution of relays and 2) the distribution of IUSNs, so the optimal ERM selection can be determined. Clearly, if an USN is located far away from the USV, it must be served by AUVs to make sure that its data can be successfully collected. Therefore, with the support of AUVs, all IUSNs' data will be received, thus effectively ameliorating the response efficiency.

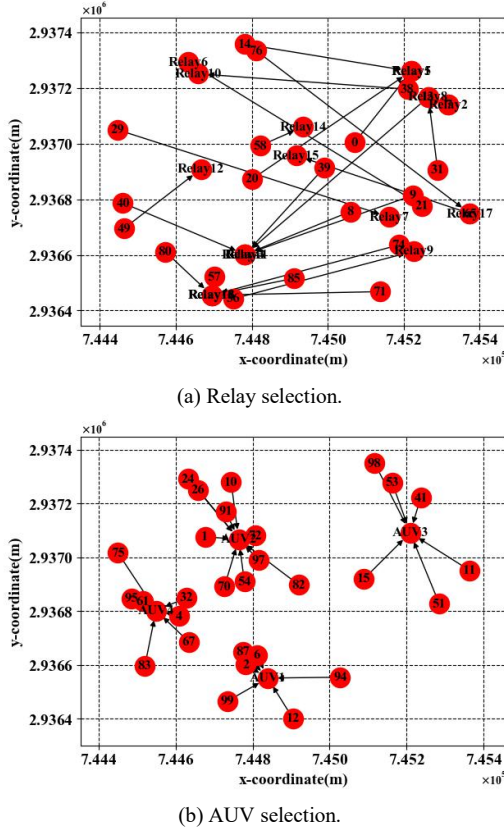


Fig. 3. Optimal ERM selection.

Fig. 4 shows the results of optimal relay selection derived from RL and KMA, respectively. As illustrated in Fig. 4(a), we present the results of average reward, namely, average channel capacity, by comparing the results derived from Q-learning, Sarsa, DQN, and KMA, respectively. The average reward of Q-learning gives better performance (3781.91 kbps) compared with Sarsa (3523.12 kbps), DQN (1911.97 kbps), and KMA (783.50 kbps). In Fig. 4(b), we can find that the average reward of our approach is equal to 5095.06 kbps by combining the results derived from Algorithm 2 and 3. As a result, 23 USNs

are determined by \bar{R} in (30) to transmit data to relays, namely, the USNs in *ERM 1*, as shown in Fig. 4(c). Therefore, given the fixed packet size, our approach can dramatically shorten the amount of time for data transmission, and the number of USNs served by AUVs, namely, IUSNs, can be also reduced effectively, which further saves the working time and energy consumption of AUVs.

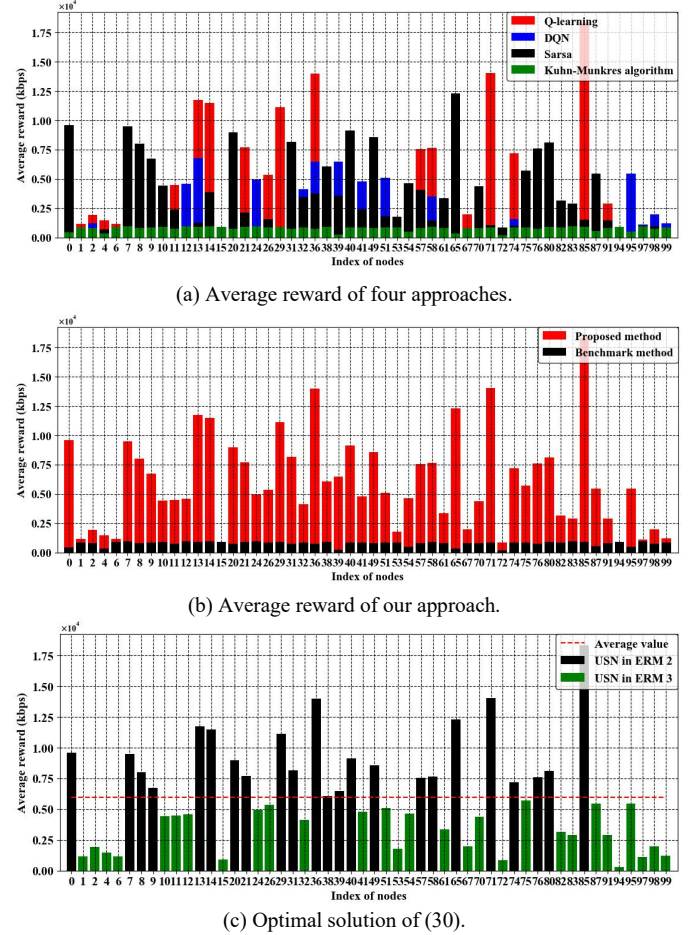
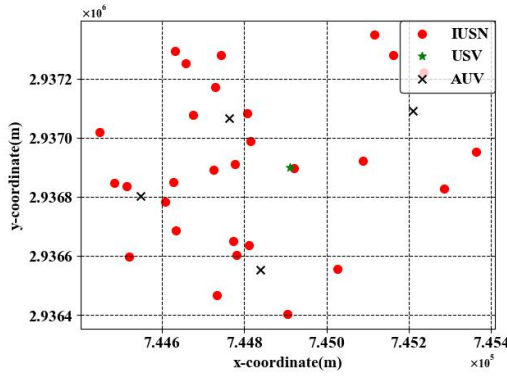
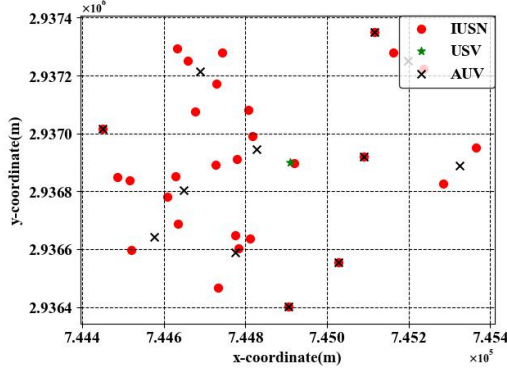


Fig. 4. Optimal relay selection.

Fig. 5 shows the results of optimal AUV deployment, i.e., AUVs leave the USV and update their three-dimension (3D) positions derived from the AKMC by minimizing the UCL path loss between AUVs and IUSNs, and maximizing the AUV velocity, respectively. As shown in Fig. 5, each AUV arrives at its optimal suspension position to maximize the UCL channel capacity, and IUSNs will forward data to AUVs according their cluster labels. Compared with the traditional KMC (the number of cluster-heads are given in advance) and MSC (the number of cluster-heads are determined adaptively) (see Fig. 5(b)), we propose an AKMC to determine the optimal number of cluster-heads without prior knowledge. From Fig. 5(a), we can see that the cluster-heads derived from AKMC is equal to 4, but the result of MSC equals 11. Moreover, the velocity of each AUV is also optimized by (49), subject to a given set of serving capacity and energy constraints, thus improving the response efficiency.



(a) Clustering result of AKMC.

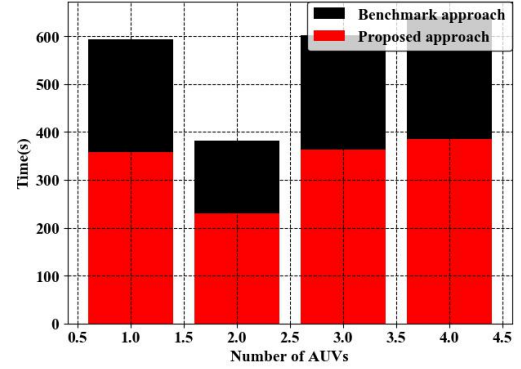


(b) Clustering result of MSC.

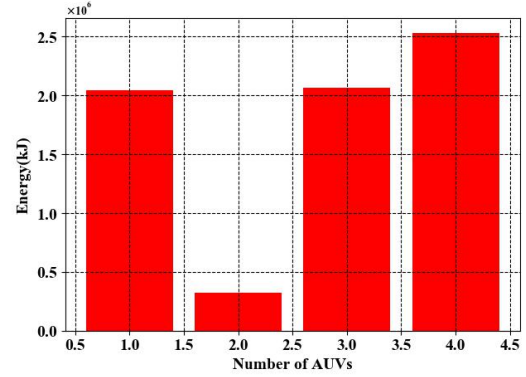
Fig. 5. Optimal AUV deployment.

In Fig. 6, we present the best tradeoff between response efficiency and energy consumption. As mentioned in (62)-(63), we need to determine the optimal number of AUVs, namely, the input of KMC, and the optimal transmit power of IUSNs to simultaneously minimize the total amount of time and the total energy consumption of underwater communication and motion. It is well known that the PF of (69) consists of many sparse sub-optimal points and the reference vector $\mathbf{z}^* = (z_1^*, z_2^*)$ satisfies an uniform distribution generated by the *Das-Dennis method* [43]. According to the sparsity and the convergence of the PF, we determine the PO by the weights derived from (71), and the best tradeoff point is selected as the PO. Thus, the optimal solution of (69) is also determined. Since (62) is a MMP, the optimal time of emergency response depends on the maximum of AUV working time. In contrast, (63) is a minimization problem, so the optimal solution of (63) depends on the cumulative sum of energy consumed by all AUVs. Specifically, as shown in Fig. 6(a), we can see that the optimal number of AUVs derived from Algorithm 4 is equal to 4. Here, 4 AUVs are simultaneously dispatched to collect emergency data, and the amount of time for emergency response depends on AUV 4, i.e., the optimal response efficiency equals 387 s, thus reducing 36% of the amount of time. However, from Fig. 6(b), we can know that the optimal energy consumption equals 6.7×10^6 kJ, which is the sum of energy consumption of 4 AUVs. Extremely, we can image that if just one AUV is used, the energy consumption might exceed its energy limitation. Moreover, as shown in Fig. 6(c), we express the energy efficiency as the total energy consumption divided by response

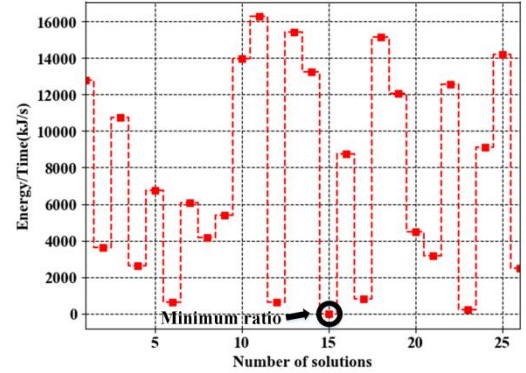
efficiency, and the best solution is obtained by searching the solution with the minimum ratio. Consequently, the energy-efficient UECN can be established.



(a) Response efficiency.



(b) Energy consumption.



(c) Energy-efficient solutions.

Fig. 6. Optimal solution of OP.

V. CONCLUSION

To realize energy-efficient underwater emergency response, this article established an UECN to collect and transmit underwater emergency data. We first determined the optimal ERM for each USN by hierarchical segmentation, including relay detection and selection. Specifically, the relays were found out by greedy searching, and the best strategy of relay selection was trained, which ensured the connectivity between USNs and relays, and also compensated the energy limitation of AUVs. Next, based on the distribution of IUSNs, we scheduled AUVs to assist IUSNs in collecting emergency data by jointly updating the position and control of each AUV,

where the optimal UCL channel capacity and the maximum velocity were obtained, which effectively saved the amount of time for underwater communication and moving. The simulation results demonstrated that the proposed approach saved 36% of emergency response time, and could make some contributions to underwater emergency response.

However, there are some potential problems that are not addressed in this article, which are worthy of in-depth discussion in our future works. Firstly, it is challenging to establish an UECN in an unknown environment. Since users can move randomly, the support of mobile data collection is vital, which requires the development of access and control protocols of underwater internet of things (UIoT). Secondly, according to different receiver types, it is useful to realize the highly effective handover and load balancing. To ensure the connectivity of underwater backhaul networks, the pointing of network traffic dynamically varies, which needs precise synchronization. Moreover, the adaptive link switching in a hybrid system needs extra attention, and the effective hybrid transmission (e.g., VLC/optical camera communication (OCC) or light fidelity (LiFi)/VLC) is also worth being investigated.

REFERENCE

- [1] R. W. L. Coutinho, A. Boukerche, L. F. M. Vieira, and A. A. F. Loureiro, "Underwater Sensor Networks for Smart Disaster Management," *IEEE Consumer Electronics Magazine*, vol. 9, no. 2, pp. 107-114, 2020.
- [2] J. Harmouche and S. Narasimhan, "Long-Term Monitoring for Leaks in Water Distribution Networks Using Association Rules Mining," *IEEE Transactions on Industrial Informatics*, vol. 16, no. 1, pp. 258-266, 2020.
- [3] N. Zhao et al., "UAV-assisted emergency networks in disasters," *IEEE Wireless Communications*, vol. 26, no. 1, pp. 45-51, 2019.
- [4] Z. Huang, C. Chen, and M. Pan, "Multiobjective UAV Path Planning for Emergency Information Collection and Transmission," *IEEE Internet of Things Journal*, vol. 7, no. 8, pp. 6993-7009, 2020.
- [5] J. Wang, W. Cheng, and H. Zhang, "Statistical QoS Provisioning Based Caching Placement for D2D Communications Based Emergency Networks," in *IEEE INFOCOM 2020 - IEEE Conference on Computer Communications Workshops (INFOCOM WKSHPS)*, 2020, pp. 449-454.
- [6] M. Samir, S. Sharafeddine, C. M. Assi, T. M. Nguyen, and A. Ghayeb, "UAV Trajectory Planning for Data Collection from Time-Constrained IoT Devices," *IEEE Transactions on Wireless Communications*, vol. 19, no. 1, pp. 34-46, 2020.
- [7] P. K. Sajmath, R. V. Ravi, and K. K. A. Majeed, "Underwater Wireless Optical Communication Systems: A Survey," in *2020 7th International Conference on Smart Structures and Systems (ICSSS)*, 2020, pp. 1-7.
- [8] N. Saeed, A. Celik, T. Y. Al-Naffouri, and M.-S. Alouini, "Underwater optical wireless communications, networking, and localization: A survey," *Ad Hoc Networks*, vol. 94, p. 101935, 2019/11/01/ 2019.
- [9] M. Z. Chowdhury, M. K. Hasan, M. Shahjalal, M. T. Hossan, and Y. M. Jang, "Optical Wireless Hybrid Networks: Trends, Opportunities, Challenges, and Research Directions," *IEEE Communications Surveys & Tutorials*, vol. 22, no. 2, pp. 930-966, 2020.
- [10] T. Qiu, Z. Zhao, T. Zhang, C. Chen, and C. L. P. Chen, "Underwater Internet of Things in Smart Ocean: System Architecture and Open Issues," *IEEE Transactions on Industrial Informatics*, vol. 16, no. 7, pp. 4297-4307, 2020.
- [11] M. Elamassie and M. Uysal, "Vertical Underwater Visible Light Communication Links: Channel Modeling and Performance Analysis," *IEEE Transactions on Wireless Communications*, pp. 1-1, 2020.
- [12] A. Celik, N. Saeed, B. Shihada, T. Y. Al-Naffouri, and M. Alouini, "End-to-End Performance Analysis of Underwater Optical Wireless Relaying and Routing Techniques Under Location Uncertainty," *IEEE Transactions on Wireless Communications*, vol. 19, no. 2, pp. 1167-1181, 2020.
- [13] P. K. W. S. H. A. Suraweera, R. I. Godaliyadda, V. R. Herath, and Z. Din, "Impact of Receiver Orientation on Full-Duplex Relay Aided NOMA Underwater Optical Wireless Systems," in *ICC 2020 - 2020 IEEE International Conference on Communications (ICC)*, 2020, pp. 1-7.
- [14] B. Shihada et al., "Aqua-Fi: Delivering Internet Underwater Using Wireless Optical Networks," *IEEE Communications Magazine*, vol. 58, no. 5, pp. 84-89, 2020.
- [15] J. Huang and R. Diamant, "Adaptive Modulation for Long-Range Underwater Acoustic Communication," *IEEE Transactions on Wireless Communications*, vol. 19, no. 10, pp. 6844-6857, 2020.
- [16] A. A. Al-habob and O. A. Dobre, "Role Assignment for Energy-Efficient Data Gathering Using Internet of Underwater Things," in *ICC 2020 - 2020 IEEE International Conference on Communications (ICC)*, 2020, pp. 1-6.
- [17] Y. Song, "Underwater Acoustic Sensor Networks With Cost Efficiency for Internet of Underwater Things," *IEEE Transactions on Industrial Electronics*, vol. 68, no. 2, pp. 1707-1716, 2021.
- [18] P. Saini, R. P. Singh, and A. Sinha, "Path loss analysis of RF waves for underwater wireless sensor networks," in *2017 International Conference on Computing and Communication Technologies for Smart Nation (IC3TSN)*, 2017, pp. 104-108.
- [19] K. G. Omeke, A. Abohmra, M. A. Imran, Q. H. Abbasi, and L. Zhang, "Characterization of RF signals in different types of water," in *Antennas and Propagation Conference 2019 (APC-2019)*, 2019, pp. 1-6.
- [20] S. M. Maher, Z. M. Ali, H. H. Mahmoud, S. O. Abdellatif, and M. M. Abdellatif, "Performance of RF underwater communications operating at 433 MHz and 2.4 GHz," in *2019 International Conference on Innovative Trends in Computer Engineering (ITCE)*, 2019, pp. 334-339.
- [21] N. Farr, A. Bowen, J. Ware, C. Pontbriand, and M. Tivey, "An integrated, underwater optical /acoustic communications system," in *OCEANS'10 IEEE SYDNEY*, 2010, pp. 1-6.
- [22] L. J. Johnson, R. J. Green, and M. S. Leeson, "Hybrid underwater optical/acoustic link design," in *2014 16th International Conference on Transparent Optical Networks (ICTON)*, 2014, pp. 1-4.
- [23] M. Soomro, S. N. Azar, O. Gurbuz, and A. Onat, "Work-in-Progress: Networked Control of Autonomous Underwater Vehicles with Acoustic and Radio Frequency Hybrid Communication," in *2017 IEEE Real-Time Systems Symposium (RTSS)*, 2017, pp. 366-368.
- [24] C. Lin, G. Han, M. Guizani, Y. Bi, J. Du, and L. Shu, "An SDN Architecture for AUV-Based Underwater Wireless Networks to Enable Cooperative Underwater Search," *IEEE Wireless Communications*, vol. 27, no. 3, pp. 132-139, 2020.
- [25] S. Chen, Y. Chen, J. Zhu, and X. Xu, "Path-Planning Analysis of AUV-Aided Mobile Data Collection in UWA Cooperative Sensor Networks," in *2020 IEEE International Conference on Signal Processing, Communications and Computing (ICSPCC)*, 2020, pp. 1-5.
- [26] G. Han, X. Long, C. Zhu, M. Guizani, and W. Zhang, "A High-Availability Data Collection Scheme based on Multi-AUVs for Underwater Sensor Networks," *IEEE Transactions on Mobile Computing*, vol. 19, no. 5, pp. 1010-1022, 2020.
- [27] Y. Su, M. Liwang, Z. Gao, L. Huang, X. Du, and M. Guizani, "Optimal Cooperative Relaying and Power Control for IoUT Networks With Reinforcement Learning," *IEEE Internet of Things Journal*, vol. 8, no. 2, pp. 791-801, 2021.
- [28] F. Xing, H. Yin, X. Ji, and V. C. M. Leung, "Joint Relay Selection and Power Allocation for Underwater Cooperative Optical Wireless Networks," *IEEE Transactions on Wireless Communications*, vol. 19, no. 1, pp. 251-264, 2020.
- [29] J. V. Aravind, S. Kumar, and S. Prince, "Mathematical Modelling of Underwater Wireless Optical Channel," in *2018 International Conference on Communication and Signal Processing (ICCSP)*, 2018, pp. 0776-0780.
- [30] P. Daegil, K. Jinhyun, and C. Wan Kyun, "Simulated 3D underwater localization based on RF sensor model using EKF," in *2011 8th International Conference on Ubiquitous Robots and Ambient Intelligence (URAI)*, 2011, pp. 832-833.
- [31] A. Goldsmith, *Wireless communications*. Cambridge university press, 2005.
- [32] J. Cao, J. Cao, Z. Zeng, and L. Lian, "Optimal path planning of underwater glider in 3D dubins motion with minimal energy consumption," in *OCEANS 2016 - Shanghai*, 2016, pp. 1-7.
- [33] S. Zhang, J. Yu, A. Zhang, and F. Zhang, "Spiraling motion of underwater gliders: Modeling, analysis, and experimental results," *Ocean Engineering*, vol. 60, pp. 1-13, 2013/03/01/ 2013.
- [34] Y. Deng, Y. Chen, Y. Zhang, and S. Mahadevan, "Fuzzy Dijkstra algorithm for shortest path problem under uncertain environment," *Applied Soft Computing*, vol. 12, no. 3, pp. 1231-1237, 2012.

- [35] C. H. Liu, Z. Chen, J. Tang, J. Xu, and C. Piao, "Energy-Efficient UAV Control for Effective and Fair Communication Coverage: A Deep Reinforcement Learning Approach," *IEEE Journal on Selected Areas in Communications*, vol. 36, no. 9, pp. 2059-2070, 2018.
- [36] J. Xiong et al., *Parametrized Deep Q-Networks Learning: Reinforcement Learning with Discrete-Continuous Hybrid Action Space*. 2018.
- [37] S. Adam, L. Busoniu, and R. Babuska, "Experience Replay for Real-Time Reinforcement Learning Control," *IEEE Transactions on Systems, Man, and Cybernetics, Part C (Applications and Reviews)*, vol. 42, no. 2, pp. 201-212, 2012.
- [38] S. Zhou, X. Liu, Y. Xu, and J. Guo, "A Deep Q-network (DQN) Based Path Planning Method for Mobile Robots," in *2018 IEEE International Conference on Information and Automation (ICIA)*, 2018, pp. 366-371.
- [39] M. Mozaffari, W. Saad, M. Bennis, and M. Debbah, "Mobile Unmanned Aerial Vehicles (UAVs) for Energy-Efficient Internet of Things Communications," *IEEE Transactions on Wireless Communications*, vol. 16, no. 11, pp. 7574-7589, 2017.
- [40] K. L. Wu and M. S. Yang, "Mean shift-based clustering," *Pattern Recognition*, vol. 40, no. 11, pp. 3035-3052, 2007.
- [41] Q. Zhang and H. Li, "MOEA/D: A multiobjective evolutionary algorithm based on decomposition," *IEEE Transactions on evolutionary computation*, vol. 11, no. 6, pp. 712-731, 2007.
- [42] K. Deb, "Multi-objective Optimisation Using Evolutionary Algorithms: An Introduction," in *Multi-objective Evolutionary Optimisation for Product Design and Manufacturing*, L. Wang, A. H. C. Ng, and K. Deb, Eds. London: Springer London, 2011, pp. 3-34.
- [43] L. Rachmawati and D. Srinivasan, "Multiobjective Evolutionary Algorithm With Controllable Focus on the Knees of the Pareto Front," *IEEE Transactions on Evolutionary Computation*, vol. 13, no. 4, pp. 810-824, 2009.
- [44] F. Xing, H. Yin, Z. Shen, and V. C. M. Leung, "Joint Relay Assignment and Power Allocation for Multiuser Multirelay Networks Over Underwater Wireless Optical Channels," *IEEE Internet of Things Journal*, vol. 7, no. 10, pp. 9688-9701, 2020.
- [45] H. Zhu, M. Zhou, and R. Alkins, "Group Role Assignment via a Kuhn-Munkres Algorithm-Based Solution," *IEEE Transactions on Systems, Man, and Cybernetics - Part A: Systems and Humans*, vol. 42, no. 3, pp. 739-750, 2012.